Journal of the European Ceramic Society 22 (2002) 1783–1790

www.elsevier.com/locate/jeurceramsoc

Corrosion of spinel clinker by $CaO–Al_2O_3–SiO_2$ ladle slag

Mun-Kyu Cho*, Gi-Gon Hong, Seok-Keun Lee

High Temperature Refractory Materials Research Team, Materials and Processes Research Center, Research Institute of Industrial Science and Technology(RIST), PO Box 135, Pohang 790-600, South Korea

Received 8 May 2001; received in revised form 5 November 2001; accepted 17 November 2001

Abstract

Three different grades of sintered spinel clinker were used containing 47, 69 and 94 wt.% Al_2O_3, respectively, i.e. MgO-rich, stoichiometric and Al_2O_3-rich. Based on these clinkers, the corrosion mechanism of each spinel clinker by $CaO–Al_2O_3–SiO_2$ slag was investigated and the corrosion and penetration behavior of castables containing powdered spinel clinker examined. A layer of $MgO·(Al, Fe)_2O_3$ complex spinel formed at the slag-refractory interface was proportional to the MgO content of the spinel clinkers, and it depressed the slag corrosion. The free MgO and spinel minerals in each spinel clinker mainly trapped Fe_2O_3 from the slag. $CaO–Al_2O_3$ compounds were formed at the slag-clinker interface by the reaction between free Al_2O_3 in the Al_2O_3-spinel clinker and CaO from slag. Slag penetration into the spinel clinkers was retarded by these compounds. As a result of adding fine spinel powder to the matrix of Al_2O_3-based castables, it was observed that higher content of MgO in spinel clinker showed better resistance to slag corrosion but lower resistance to slag penetration. © 2002 Published by Elsevier Science Ltd.

Keywords: Al_2O_3–spinel; Castable; Corrosion; Refractories; Slag; Spinel

1. Introduction

Recently the application of monolithic refractories to teeming ladles has been rapidly increased. At first the major material for castables were based on the zircon-silica system. However, recently alumina-spinel and alumina-magnesia systems have become popular due to demand for clean molten steel, the increment in secondary refining.

Alumina-spinel castables with a calcium-aluminate-derived bond contain 10–25% $MgO·Al_2O_3$ on the basis of Al_2O_3 as a major material. The spinel in this system traps FeO from the slag, thus suppressing slag penetration, while alumina reacts with CaO of slag compositions to form solid compounds such as $CaO·6Al_2O_3$.[1] As a result, the residual molten slag becomes SiO_2-rich with high viscosities. Therefore, the slag penetration within castables is suppressed. Alumina-magnesia castables contain MgO instead of the spinel of alumina-spinel castables. During usage the matrix in this system is strengthened due to spinel formed by the reaction between MgO and Al_2O_3, and the corrosion resistance of castables is improved.[1,2]

Extensive studies of the effects of spinel clinker compositions on alumina-spinel castable properties have been carried out. Takano et al.[3] prepared alumina-rich ($\geqslant$90 wt.%) spinel clinker in which corundum coexisted. When the clinkers were used as aggregates in the castables, the corrosion of castables was suppressed. Also, when used as part of the fine matrix of the castables, it was effective in preventing slag penetration. In castables using spinel clinkers with various MgO contents(5–50 wt.%) as aggregates and matrix, Nagasoe et al.[4] reported that the specimen containing spinel clinker with about 20 wt.% MgO was the most resistant to slag penetration. Meanwhile, in the specimen containing spinel clinker with 5 wt.% MgO, large cracks were formed by the formation of $CA_2(CaO·2Al_2O_3)$ and $CA_6(CaO·6Al_2O_3)$.

Lee and Zhang[5] reviewed the penetration and dissolution mechanisms for refractories. This review has highlighted two types of attack (direct and indirect) of refractories by silicate liquids. They concluded that control of slag attack could be through the refractory whose composition was arranged to make the local liquid viscous by uptake or release of suitable species or

* Corresponding author.
E-mail address: kyumc@lycos.co.kr (M.-K. Cho).

0955-2219/02/$ - see front matter © 2002 Published by Elsevier Science Ltd.
PII: S0955-2219(01)00509-X

by development of a tight texture and/or dense layers at the liquid/refractory interface.

Chen and Ko[6] reported that hot modulus of rupture values of Al_2O_3-spinel castables containing Al_2O_3-rich spinel (10 wt.% MgO) were significantly higher than those of Al_2O_3 castable without spinel addition. They concluded that the enhancement of hot strength in Al_2O_3-spinel castables was due to the strong interlocking bond between the CA_6 and spinel grains. Korgul et al.[7] reported that MgO-rich spinel-alumina castables underwent less corrosion as dissolution of MgO led to a viscous MgO-rich slag which was less corrosive to the Al_2O_3 component of the refractory.

However, slag compositions vary greatly between steelwork and even between batches at the same works, so that the corrosion behaviour of a refractory may vary significantly. Considering this aspect, the effects of grades of spinel clinker on the basic reaction between slag and spinel clinker influence strongly the corrosion mechanism of alumina-spinel castables. Therefore, in this study three different grades of sintered spinel clinker were used containing 47, 69 and 94 wt.% Al_2O_3, respectively, i.e. MgO-rich, stoichiometric and Al_2O_3-rich, the stoichiometric amount of Al_2O_3 in spinel being 71.67 wt.%. Based on these clinkers, the corrosion mechanism of each spinel clinker by $CaO–Al_2O_3–SiO_2$ slag was investigated and the corrosion and penetration behavior of castables containing each spinel clinker as a powder in its matrix system were examined.

2. Experimental procedure

The chemical composition, bulk density, apparent porosity and mineral phases of three different grades of sintered spinel clinker and slag were listed in Table 1. All spinel clinkers were from Onoda. Each spinel clinker was designated by S-50, S-70 and S-90, where the first letter, S, indicated spinel and numbers stood for Al_2O_3 content of spinel clinker. Bulk density and porosity were determined by the Archimedes method using water as an immersion medium. The ladle slag was a typical commercial composition (POSCO, Pohang Iron and Steelmaking Co.) used in this study was crushed and sieved below 200 mesh. Also, equivalently sized spinel clinkers (i.e. 5 mm) were selected in order to give consistent change of slag composition by dissolution of spinel during reaction.

The spinel clinkers were buried in slag powders (20 g) and charged into an alumina crucible (50×40×10(t) mm) for heat treatment in air at 1500 and 1600 °C for 5 min using electric furnace (250×250×350 mm). The purity of alumina crucible was above 99.9%. After natural cooling, spinel clinkers reacted with slag were prepared by cutting alumina crucible to observe post-mortem microstructures in an attempt to elucidate the corrosion mechanism. All samples were polished, gold-coated and examined in backscattered and secondary electron imaging mode on a Jeol 840A scanning electron microscope (SEM). Concentrations of Al, Mg, Ca, and so on were obtained from the measured X-ray intensities by calibration with EDAX ZAF quantification (standardless).

The castable formulation (Table 2) was chosen to examine the resistance to slag corrosion and penetration. Three different grades of sintered spinel were used as fine parts. Batches were dry-mixed before adding water and wet mixing for 5 min with water of 6.5 wt.%. Sodium hexameta-phosphate of 0.1 wt.% was added to all batches as a deflocculant. The mixed materials was vibration-cast into 40×160×20 mm stainless steel moulds. Vibration time was 5 min at a frequency of 70 Hz. Samples were cured in air at ambient temperature for 24 h. After mould removal samples were dried at 110 °C for 24 h. All castables were given a high-frequency induction melting furnace test at 1650 °C for 2 h using ladle slag with the composition given in Table 1. The test was carried out at two cycles. One cycle was to hold for an hour. Ladle slag and steel were used. Refractory samples were set in the shape of a polygonal crucible in the induction furnace. Slag was added when the molten steel had reached the test temperature of 1650 °C. For the corroded amount, the maximum corroded area on the boundary between slag and metal was measured. In the measurement of the amount of corrosion and penetration, each specimen was cut longitudinally at three positions and the average of corroded and faded dimensions was calculated. Its result was

Table 1
Chemical compositions, mineral phases, density and porosity of spinel clinkers and slag (wt%)

	Chemical composition (wt.%)						Mineral phases	Bulk density	Porosity (%)
	SiO_2	Al_2O_3	CaO	MgO	Fe_2O_3	others			
S-50	0.38	46.69	0.70	50.76	0.19	1.28	Spinel, periclase	3.30	2.80
S-70	0.25	69.12	0.42	29.30	0.17	0.74	Spinel, periclase* (*minor)	3.19	2.95
S-90	0.12	93.59	–	5.77	0.07	0.45	Spinel, corundum(α-Al_2O_3)	3.42	2.31
Slag	7.52	30.65	39.84	5.54	13.10	3.35	$C_{12}A_7$*, CA_2, Gehlenite (C_2AS) (C = CaO, A = Al_2O_3, S = SiO_2) (*major)	–	–

Table 2
Castable compositions (wt.%)

Type	Properties	A	B	C
Aggregate alumina	−5 mm, ⩾99%	67	67	67
Fine powder				
S-50	−0.074 mm	15		
S-70	−0.074 mm		15	
S-90	−0.074 mm			15
Alumina	−0.074 mm, ⩾99%	8	8	8
Alumina cement	−0.074 mm, Al_2O_3 80%	10	10	10

shown as a relative index on the basis of specimen A. The corrosion/penetration indices are given by the equation:

$$\text{Corrosion Index} = \frac{\text{amount of corrosion of specimen}}{\text{amount of corrosion of specimen A}} \times 100 \quad (1)$$

$$\text{Penetration Index} = \frac{\text{amount of penetration of specimen}}{\text{amount of penetration of specimen A}} \times 100 \quad (2)$$

3. Results and discussion

Fig. 1 shows backscattered SEM images of the spinel clinkers. In MgO-rich spinel clinker (S-50), stoichiometric spinel co-existed with periclase and secondary phases were not observed at grain boundaries. In sub-stoichiometric spinel clinker (S-70), stoichiometric spinel co-existed with fine periclase as minor phase and the secondary phase was observed at grain boundaries, which had the composition of $CaO:MgO:SiO_2 = 29.3:28.3:42.4$ as revealed by EDS. Al_2O_3-rich spinel clinker (S-90) consisted of corundum and sub-stoichiometric spinel which had the composition of $MgO:Al_2O_3 = 21:79$ as revealed by EDS, with no secondary phases at the grain boundaries.

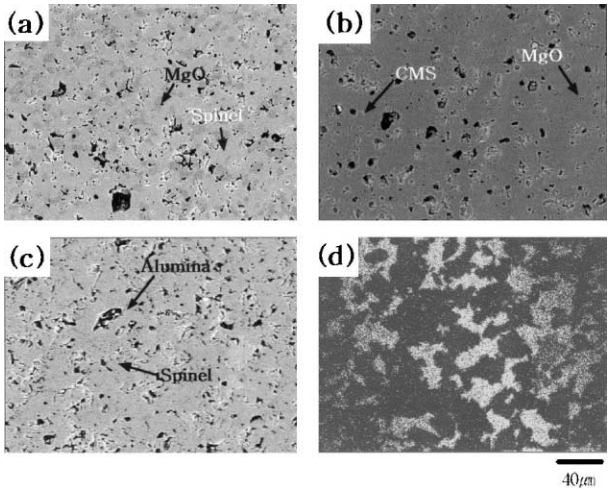

Fig. 1. Back scattered electron images of specimens of (a) S-50 spinel, (b) S-70 spinel and (c) S-90 spinel clinker, (d) Mg X-ray dot map of (c).

Figs. 2, 3, 4 and Table 3 show the slag-clinker interfaces and quantitative EDS analysis with the polished cross sections of specimens reacted with slag at 1500 °C for 5 min.

Comparison of the composition of slag adhered to MgO-rich spinel clinker (points 1 and 2 in Table 3) with that of the as-received slag indicated that no MgO in this clinker dissolved into the slag. The formation of complex spinel, $MgO\cdot(Al, Fe)_2O_3$ (point 3 in Table 3), was observed at the surface of the spinel clinkers, which had been in contact with the slag. Since there was no MgO dissolution into the slag, it was considered that the complex spinel was produced by reaction of MgO–Al_2O_3 spinel with FeO/Fe_2O_3 in the slag or $MgO\cdot Al_2O_3$ spinel with MgO–FeO phase, which arose from reaction of free MgO in the spinel with FeO/Fe_2O_3 in the slag. This suggests that the FeO/Fe_2O_3 in slag was trapped by MgO grain, shown in point 6 in Table 3, leading to formation of MgO–FeO phases. The EDS line analyses of the spinel clinker are shown in Fig. 2. It was apparent that the penetration of Ca and Si was deeper than that of Fe and Mn, while the concentration of Ca and Si was lower than that of Fe and Mn at the slag/clinker interface. Also, the dissolution of grains in spinel clinker into slag did not occur at the slag/clinker interface.

As shown in Fig.3, the microstructure of stoichiometric spinel clinker after corrosion test was almost the same as that of MgO-rich spinel clinker. However, the layer of complex spinel (labeled a and b in Fig. 3) was thinner (20–25 μm) and the penetration of Fe/Ca/Si components was greater, compared with MgO-rich spinel (40–50 μm). The above results indicate MgO was better trapping Fe-oxide than spinel. Fig. 3 reveals that grain growth of $MgO\cdot(Al,Fe)_2O_3$ complex spinel occurred at the slag-clinker interface. This grain growth can be explained by the content of FeO/Fe_2O_3, which becomes greater near the slag/clinker interface (labeled a–c in Fig. 3). In the phase diagram of the MgO–Fe_2O_3 system,[8] the melting point of MgO–Fe_2O_3 decreases with increasing Fe_2O_3 content, which enhances the sinterability of $MgO\cdot(Al,Fe)_2O_3$ complex spinel with the aid of more fluid liquid.

Fig. 4 reveals that penetration of slag into the Al_2O_3-rich spinel clinker is limited. This result can be explained by the formation of CaO–Al_2O_3 phases (point 15 in Fig. 4 and labeled 15 in Table 3) at the slag-clinker interface. The CaO in the slag reacts with Al_2O_3 (especially free Al_2O_3) of the spinel clinker so that the slag saturates in Al_2O_3 and increases its viscosity and melting temperature limiting slag penetration.[9] As a result, the CaO–Al_2O_3 compounds such as $CaO\cdot 2Al_2O_3$ and

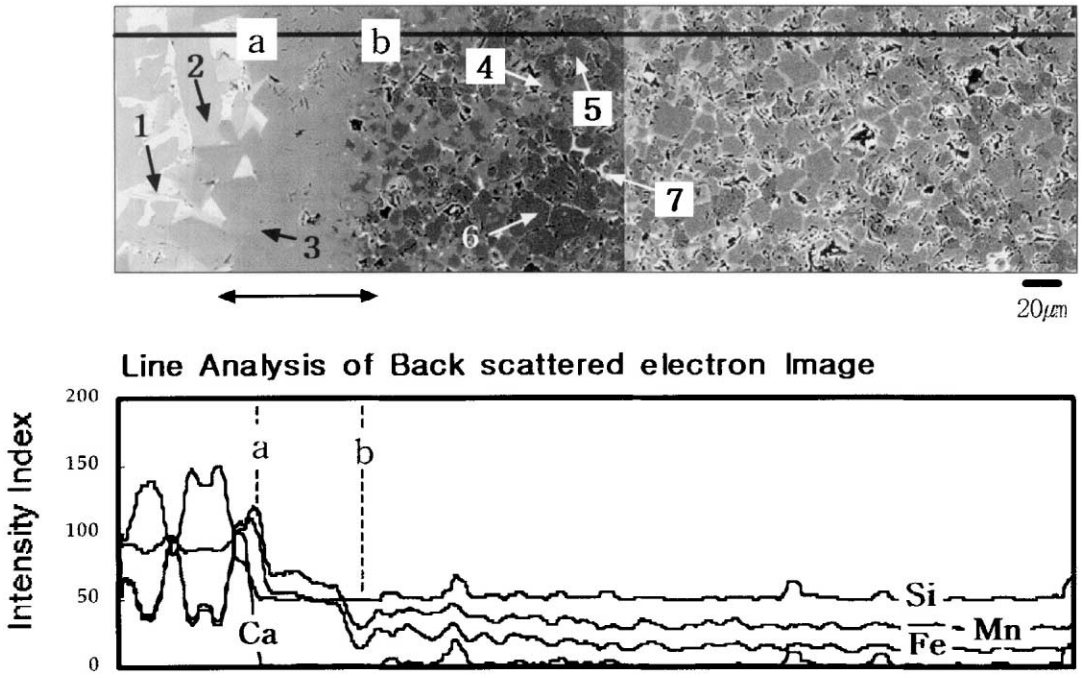

Fig. 2. Back scattered electron image and line analysis of the slag/clinker interface of S-50 spinel clinker from corrosion layer to original layer after slag corrosion test at 1500 °C for 5 min.

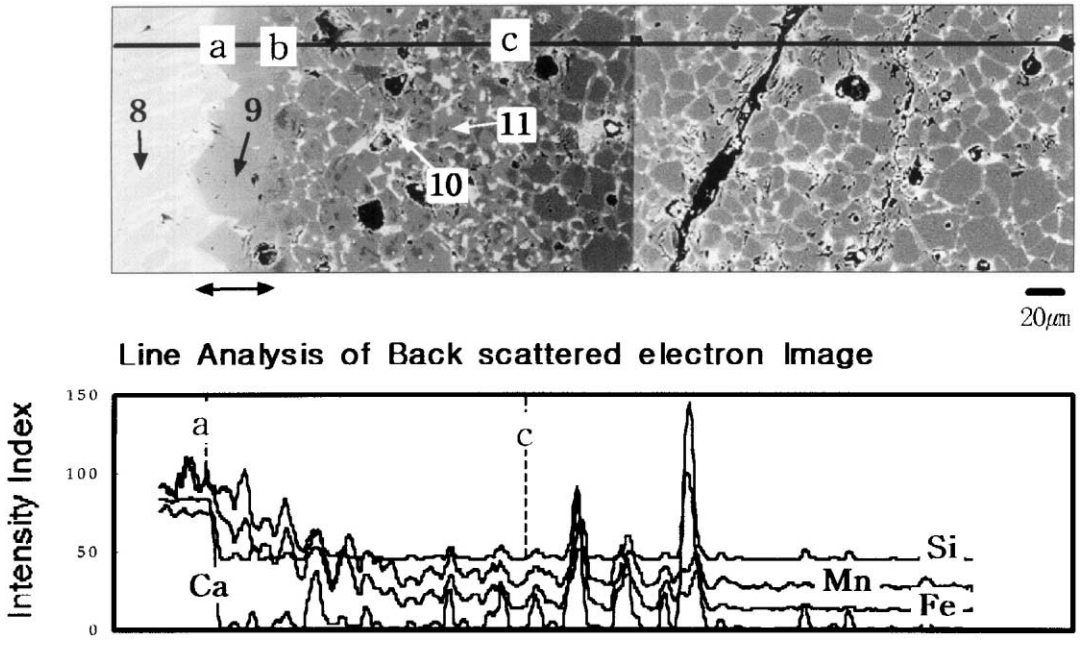

Fig. 3. Back scattered electron image and line analysis of the slag/clinker interface of S-70 spinel clinker from corrosion layer to original layer after slag corrosion test at 1500 °C for 5 min.

$CaO{\cdot}6Al_2O_3$ at the slag-clinker interface are precipitated. Also, some spinel grains dissolved into the slag due to dissolution of free Al_2O_3 mainly trapedp Fe-oxide, as shown in point 13 of Fig. 4.

Fig. 5 shows a higher magnification image and EDS data of the interface between the altered layer and original layer of Fig. 2. $MgO–Fe_2O_3$ (point D) and the $MgO{\cdot}(Al,Fe)_2O_3$ complex spinel (point C) were found at original MgO location of as-received clinker. Also, spinel grain (point B) trapped FeO/Fe_2O_3 from the slag.

The formation process of phases C and D can be considered as follows. In the MgO-rich spinel clinker which had been in contact with slag, the penetration of slag occurs along the grain boundaries and pores of the

Table 3
EDS analysis (wt.%) of S-50, S-70 and S-90 clinker of Figs. 2–4

	1	2	3	4	5	6	7	8	9	10	11	12	13	14	15
MgO	1.14	2.07	23.22	25.62	25.84	91.38	6.99	1.27	24.86	1.29	24.59	1.01	24.46	1.64	1.85
Al_2O_3	11.57	34.32	58.94	66.56	73.04	3.63	18.99	12.60	68.33	11.76	67.80	12.12	67.15	38.53	72.47
SiO_2	5.65	17.41	–	–	–	–	3.81	5.11	–	5.84	–	4.07	–	8.30	–
CaO	43.63	38.01	–	–	–	–	43.12	43.50	–	42.06	–	43.10	–	39.63	21.27
TiO_2	1.80	–	–	–	–	–	–	1.74	–	1.93	–	1.04	–	–	–
MnO	2.33	–	1.67	–	–	–	1.94	2.18	0.20	2.56	–	2.05	–	–	–
Fe_2O_3	33.88	8.19	16.17	7.82	1.12	4.99	25.16	33.60	6.61	34.56	7.61	36.61	8.39	11.89	4.41

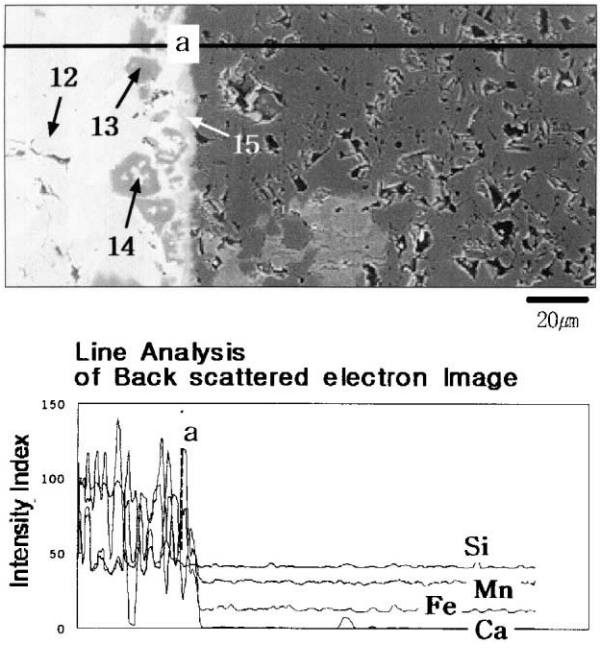

Fig. 4. Back scattered electron image and line analysis of the slag/clinker interface of S-90 spinel clinker from corrosion layer to original layer after slag corrosion test at 1500 °C for 5 min.

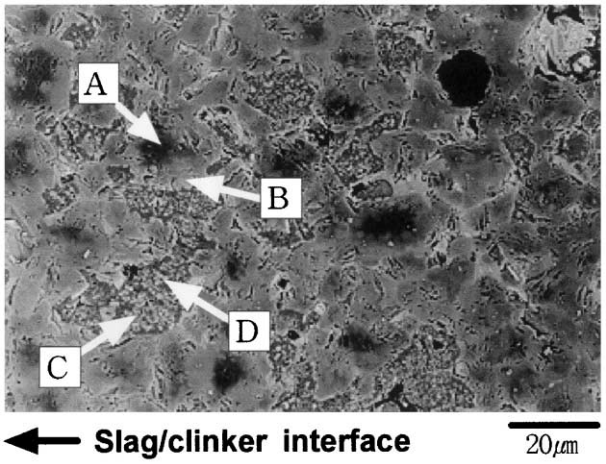

	Point A	Point B	Point C	Point D
MgO	24.7	21.8	16.5	68.2
Al_2O_3	67.4	50.0	20.5	-
MnO	-	-	3.8	4.5
Fe_2O_3	7.9	28.2	59.2	27.3

Fig. 5. Back scattered electron image and EDS result of S-50 spinel clinker after slag corrosion test at 1500 °C.

clinker and the Fe component of slag reacts preferentially with MgO grain to produce the MgO–Fe_2O_3 phases. Also, the Fe component is trapped by spinel grain through the substitution reaction of Al to Fe. This is identified by the EDS analysis of points A and B. In inner and outer parts of spinel clinker, outer part (point B) contains lower Al_2O_3 and higher Fe_2O_3 than inner part (points A) although MgO content is nearly constant. This means that the substitution reaction occurs from the outer part of spinel clinker. The free Al_2O_3 formed by the substitution reaction reacts with the MgO and MgO–Fe_2O_3 compounds to produce MgO·Al_2O_3 and MgO·(Al, Fe)$_2O_3$ complex spinel. Also, it can be considered that the MgO·(Al,Fe)$_2O_3$ complex spinel is formed by the reaction between MgO–Fe_2O_3 compounds and MgO·Al_2O_3 spinel. If free MgO does not exist (as is probable in Al_2O_3-rich spinel), the free Al_2O_3 formed by the substitution reaction between spinel and FeO/Fe_2O_3 from the slag reacts with the CaO in slag and is dissolved into the slag as CaO–Al_2O_3 compounds.

Therefore, the representative reactions between spinel clinkers and slag are the following :

$$\mathrm{MgO\ (in\ clinker)} + \mathrm{Fe_2O_3(in\ slag)} = \mathrm{MgO-Fe_2O_3\ Compounds} \quad (3)$$

$$\mathrm{MgO\cdot Al_2O_3(in\ clinker)} + y\mathrm{Fe_2O_3(in\ slag)} = \mathrm{MgO\cdot\left(Al_{1-y}Fe_y\right)_2O_3} + y\mathrm{Al_2O_3} \quad (4)$$

$$z\mathrm{MgO(free\ MgO\ in\ clinker)} + z\mathrm{Al_2O_3\,[by\ Eq.\ (4)]} = z\mathrm{MgO\cdot Al_2O_3} \quad (5)$$

$$\mathrm{MgO}-\mathrm{Fe_2O_3}\ \text{Compounds [by Eq. (3)]} + \mathrm{MgO}\cdot\mathrm{Al_2O_3}\ \text{[in clinker and by Eq. (5)]} = \mathrm{MgO}\cdot(\mathrm{Al,Fe})_2\mathrm{O_3} \quad (6)$$

$$m\mathrm{Al_2O_3}\text{[free } \mathrm{Al_2O_3} \text{ in clinker and by Eq. (4)]} + n\mathrm{CaO}\text{(in slag)} = \mathrm{Al_2O_3}-\mathrm{CaO}\ \text{Compounds} \quad (7)$$
$$(\mathrm{Al_2O_3}{:}\mathrm{CaO} = m{:}n)$$

It is considered that $MgO–Fe_2O_3$ phases are mainly produced by reaction (3) and $MgO\cdot(Al,Fe)_2O_3$ complex spinel which exists at the slag-clinker interface of MgO-rich and stoichiometric spinel is produced by reactions (4) and (6). The layer of $MgO\cdot(Al,Fe)_2O_3$ complex spinel is thicker in the MgO-rich spinel clinker than in the stoichiometric spinel clinker. This result is confirmed by the difference of MgO content in each clinker because reactions (3) and (6) depend on MgO content. It is assumed that $MgO\cdot Al_2O_3$ formed by reaction (5) inhibits the corrosion of grains at the slag/clinker interface of the MgO-rich spinel, whereas grains in Al_2O_3-rich spinel are dissolved into slag by the reaction (7).

Fig. 6 and Table 4 show the microstructure and EDS data for the spinel clinkers reacted with slag at 1600 °C for 5 min. In MgO-rich spinel, Fig. 6(a), the layer of complex spinel was being corroded at the slag–clinker interface. Also, comparison of the slag compositions adhered to the clinker treated at 1500 °C (points 1 and 2 in Table 3) with those treated at 1600 °C (points 1 and 2 in Table 4) suggests that the content of $MgO/Al_2O_3/Fe_2O_3$ in slag at 1600 °C was higher than that at 1500 °C. Also, as the temperature increased, the $MgO\cdot(Al,Fe)_2O_3$ complex spinel formed at the slag/clinker interface of the clinker at 1500 °C gradually dissolved into the slag and finally disappeared during the test. In stoichiometric spinel, Fig. 6(b), the complex spinel layer was not observed at hot face, and the spinel grains were dissolved into slag and trapped Fe-oxide from slag.

From Figs. 2, 3 and 6, it can be concluded that the thickness of the $MgO\cdot(Al,Fe)_2O_3$ complex spinel layer formed at the slag-clinker interface is determined by both the MgO content in the spinel clinker and the temperature.

Fig. 6(c) shows that penetration of slag in the Al_2O_3-rich spinel clinker was limited. Also, CaO from the slag reacted with free Al_2O_3 in the clinker so that $CaO–Al_2O_3$ compounds were precipitated at the hot face. The spinel grains were being washed away from the surface of the clinker and the dissolved spinel grains re-precipitated containing Fe-oxide from slag.

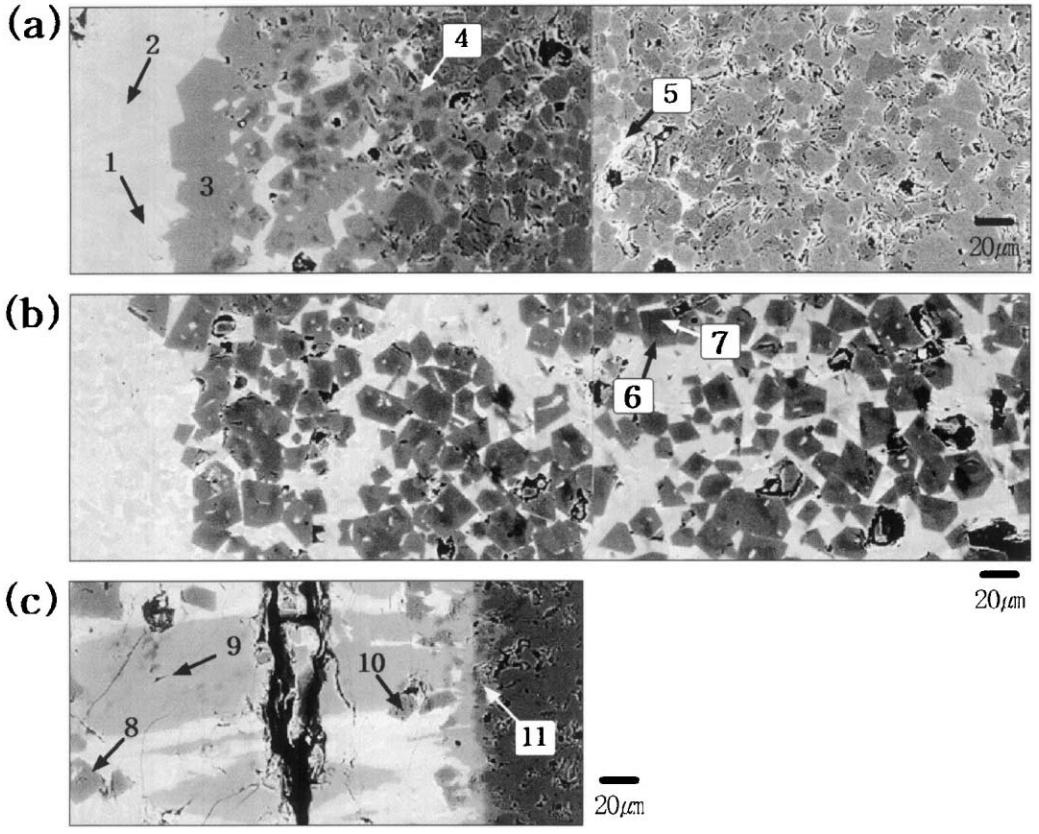

Fig. 6. Back scattered electron images of specimens of (a) S-50 spinel, (b) S-70 spinel and (c) S-90 spinel clinker from corrosion layer to original layer after slag corrosion test at 1600 °C for 5 min.

Table 4
EDS analysis (wt.%) of S-50, S-70 and S-90 clinker of Fig. 6

	1	2	3	4	5	6	7	8	9	10	11
MgO	2.00	3.62	1.27	24.85	2.50	24.23	25.82	24.10	–	23.65	3.95
Al_2O_3	13.65	36.90	11.85	63.06	28.43	67.64	73.06	60.36	73.32	68.50	88.40
SiO_2	5.70	12.14	5.78	–	2.85	–	–	–	–	–	–
CaO	42.00	37.80	43.55	–	47.45	–	–	–	22.38	–	7.65
TiO_2	1.05	–	1.90	–	2.35	–	–	–	–	–	–
MnO	1.50	–	1.29	–	–	–	–	–	–	–	–
Fe_2O_3	34.10	9.54	33.39	12.09	16.42	8.14	1.01	15.54	4.31	7.85	–

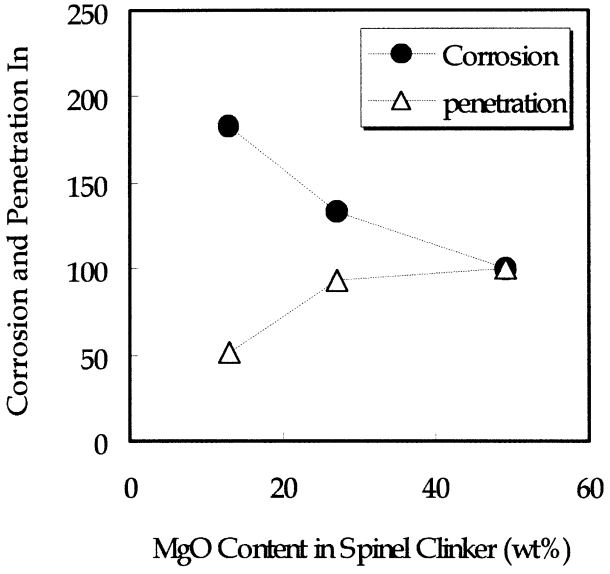

Fig. 7. Corrosion and penetration index of castables with MgO content in spinel clinker.

These results suggest that MgO-rich spinel and A_2O_3-rich spinel are desirable for slags with high Fe content and for slags having high CaO/Al_2O_3 ratio, respectively.

Fig. 7 indicates the results of corrosion test by a high frequency induction furnace method of the castable formulations shown in Table 2. The specimen using the MgO-rich spinel clinker (S50) showed the highest resistance to slag corrosion. On the contrary, the specimen using the Al_2O_3-rich spinel clinker (S90) showed the highest resistance to slag penetration, while its resistance to slag corrosion was the lowest because of its high reactivity with slag. The castable containing approx. stoichiometric spinel clinker (S70) showed higher resistance to slag corrosion and lower resistance to slag penetration, than the specimen using Al_2O_3-rich spinel (S90). These differences of the corrosion and penetration resistance between test specimens agreed with the results as previously discussed in Figs. 1, 3, 4 and 5. Also, the MgO content in a $CaO–Al_2O_3–SiO_2$ slag is known to have a critical effect on the corrosion rate of alumina-based material. The spinel with low Al_2O_3 content (i.e. MgO-rich spinel) would eventually dissolve more MgO into the slag, allowing less local dissolution of the Al_2O_3.[9] From the respect, it is considered that the corrosion resistance of the specimen using the MgO-rich spinel clinker is better than that of specimens using the stoichiometric and Al_2O_3-rich spinel.

4. Conclusion

Based on three kinds of spinel clinkers containing 47, 69 and 94 wt.% Al_2O_3, the corrosion mechanism of each spinel clinker by a $CaO–Al_2O_3–SiO_2$ ladle slag was investigated and the corrosion and penetration behavior of castables containing each spinel clinker in fine parts were examined.

1. The layer of $MgO·(Al, Fe)_2O_3$ complex spinel formed at the slag/clinker interface was proportional to the MgO content in spinel clinkers, and it depressed the direct attack of slag.
2. The free MgO and spinel minerals in each spinel clinker mainly trapped Fe_2O_3 from slag. The $CaO–Al_2O_3$ compounds were formed at slag/clinker interface by the reaction between the free Al_2O_3 in Al_2O_3-spinel clinker and the CaO from slag.
3. As a result of adding each fine spinel powder to Al_2O_3-based castables, it was observed that higher content of MgO in spinel clinker showed better resistance to slag corrosion but lower resistance to slag penetration.

References

1. Nagai, B., Matsumoto, O., Isobe, T. and Nishiumi, Y., Wear mechanism of castable for steel ladle by slag. *Taikabutsu*, 1990, **42**(8), 15–20.
2. Kobayashi, M., Kataoka, K., Sakamoto, Y. and Kifune, I., Improvement of alumina-magnesia castable for steel ladle wall. *Taikabutsu*, 1997, **49**(2), 74–80.
3. Takano, I., Shikano, H., Furusato, I., Takita, I. and Furuta, K., Effect of spinel raw material on corrosion resistance for steel ladle catable. *Taikabutsu*, 1991, **43**(4), 187–192.

4. Nagasoe, A., Tsurumoto, S. and Kitamura, A., Refractory characteristics of spinels with various MgO contents. *Taikabutsu*, 1991, **43**(1), 2–10.
5. Lee, W. E. and Zhang, S., Melt corrosion of oxide and oxide-carbon refractories. *International Materials Reviews*, 1999, **44**(3), 77–104.
6. Chan, C. F. and Ko, Y. C., Effect of CaO content on the hot strength of alumina-spinel castables in the temperature range of 1000–1500 °C. *J. Am. Ceram. Soc.*, 1998, **81**(11), 2957–2960.
7. Korgul, P., Wilson, D. R. and Lee, W. E., Microstructural analysis of corroded alumina-spinel castable refractories. *J. Eur. Ceram. Soc.*, 1997, **17**, 77–84.
8. Phillips, B., Somiya, S. and Muan, A., Melting relations of magnesium oxide-iron oxide mixtures in air. *J. Am. Ceram. Soc.*, 1961, **44**(5), 169.
9. Sandhage, K. H. and Yurek, G. J., Direct and indirect dissolution of sapphire in calcia–magnesia–alumina–silica melts : dissolution kinetics. *J. Am. Ceram. Soc.*, 1990, **73**(12), 3633–3642.